ELSEVIER

Journal of Chromatography A, 908 (2001) 131–141

JOURNAL OF CHROMATOGRAPHY A

www.elsevier.com/locate/chroma

Characterizing the performance of industrial-scale columns

John Moscariello[a], Geoff Purdom[b], Jon Coffman[c], Thatcher W. Root[a], Edwin N. Lightfoot[a,*]

[a]*Department of Chemical Engineering, University of Wisconsin–Madison, 1415 Engineering Drive, Madison, WI 53706, USA*
[b]*Millipore Corporation, 80 Ashby Road, Bedford, MA 01730, USA*
[c]*Genetics Institute, 1 Burtt Road, Andover, MA 01810, USA*

Abstract

The performance of a large commercial chromatographic column was investigated using a short pulse of a tracer and an extension of the reverse-flow technique. This technique permits separate determination of the unavoidable irreversible microscopic processes and the reversible effects of flow maldistribution, and allows for the separation of flow maldistribution in the flow distributors from flow maldistribution inside the packed bed. This analysis was performed on a 0.44 m Millipore IsoPak column using Cellufine GC 700, cellulosic-based media with an average particle diameter of 75 μm, for the stationary phase. The column efficiency was quantified by analysis of the effluent curve from a short pulse of a 5% aqueous acetone tracer. The study examined behavior of beds of different lengths (10–24 cm) and beds packed from different slurry concentrations (10–75% v/v). The slurry-packed columns were very uniform, and no significant macroscopic flow maldistribution was observed inside the column. The observed bed plate heights conformed to the predictions of available one-dimensional continuum models. Dispersion in the flow distributors was significant, corresponding to 15–25% of the intracolumn dispersion when the full 24 cm available bed length was used and a proportionally larger increase for shorter bed lengths. Thus, the headers are shown to produce a significant increase in the observed plate height.

Keywords: Preparative chromatography; Stationary phases, LC; Column performance; IsoPak columns

1. Introduction

Packing of chromatographic columns is still an art, often highly dependent upon operator skill, and no one packing technique is recognized as generally superior to all others. Packing of large industrial columns can be particularly tedious and is often poorly reproducible. Our purpose here is to characterize a commercial system, the Millipore IsoPak, which was recently developed to produce packings quickly and reproducibly for industrial scale columns. The IsoPak system uses a specialized form of slurry packing, which will be described in the Experimental section.

Our approach is to determine the efficiency of test columns for the most widely used ranges of two key operating parameters, slurry concentration of feed to the column during the packing process and final packing depth.

There is no agreement on the optimum concen-

*Corresponding author. Tel.: +1-608-262-1092; fax: +1-608-262-5434.

E-mail address: enlight@engr.wisc.edu (E.N. Lightfoot).

0021-9673/01/$ – see front matter
PII: S0021-9673(00)01062-1

tration of the particulate phase in the slurrying buffer. According to some authors, there exist optimum concentrations [1–3], while other authors only state that high slurry concentrations should be avoided [4,5]. It has been found that this variable depends on the choice of suspending buffer as well as media [6]. There has been to our knowledge no systematic investigation of the influence of packing depth on packing quality.

There has been a strong recent interest in understanding the factors that contribute to deviations from the idealized linear chromatographic models. The three most important of these factors are dispersion in peripherals, dispersion due to packing heterogeneity, and non-uniform flow from the two column flow distributors, or headers [7].

It has long been known that peripherals can cause extra-column broadening [8], and this broadening can become significant relative to the intrinsic bed broadening under some conditions. The simple statistical treatments of these extra-column contributions to the overall peak broadening are useful in correcting for these effects and characterizing the bed behavior alone [8–10]. Typically, these convolution treatments aggregate the contributions of the initial applied band width, tube volumes, dead volumes, and detector response.

Many researchers using a variety of techniques have studied the effects of packing and flow heterogeneity, and a wide variety of results have been reported. Nuclear magnetic resonance imaging, both static and dynamic [7,11–17], and direct visualization in transparent systems with refractive index solvent matching [18–20] have proven particularly effective. Significant variations in both packing density and percolating velocity have been observed, and at least in slurry-packed columns, higher than average velocities have been reported in the central regions. However, none of the above techniques can be readily applied to large columns.

The large number of patents on header design [21–30] attests to the widespread belief that headers can contribute significantly to flow maldistribution. However, little quantitative information is available, and until recently there has been no rational basis available for header design. This latter issue has been recently investigated by Yuan et al. [16], who suggested header design strategies that have been shown to give uniform flow distribution in numerical simulations and in laboratory prototypes

Development of the reverse-flow technique of probing column performance [31,32] now provides a basis for quantifying the relative effects of macroscopic flow maldistribution from the microscopic sources of dispersion described by available models, and also of separating the band broadening effects induced by header design, packing non-uniformity, and the column peripherals.

2. Theory

We will first provide the background on the one-dimensional model we use to describe the performance of an ideal column operating in differential mode, and then provide the theory to decouple the individual effects of packing heterogeneity and header maldistribution from the effects predicted from the established theory. This investigation depends upon comparison of the experimental data with predictions of a classical one-dimensional model.

2.1. Behavior of an ideal column

Our basis for analysis is the model proposed by Athalye et al. [33], which predicts the broadening of a short solute pulse as it passes through a uniformly packed chromatographic column in plug flow, as viewed on a distance scale that is large compared with particle diameter d_p. The quantitative measure of dispersion is the normalized second moment of the effluent curve with respect to the mean solute transient time [34]. When the effluent concentration profile is Gaussian, the normalized second central moment may be expressed as:

$$\overline{\mu}_2 = \left(\frac{\sigma}{\bar{t}}\right)^2 = 1/N \tag{1}$$

where σ is the standard deviation of the effluent curve normalized with respect to the mean solute residence time $\bar{t}$. In familiar terms, this second central moment is the inverse of the number of plates, N, as described by Klinkenberg and Sjenitzer [34] (see also Refs. [35,36]) for a Gaussian dis-

tribution, and the average height of a theoretical plate, H, can be expressed by $L\overline{\mu}_2$. For these idealized conditions, this simple parameter is sufficient to characterize the effluent curve.

Four microscopic factors contribute to band broadening in a packed bed of porous media: (1) intraparticle diffusion, (2) boundary layer mass transfer, (3) interparticle axial dispersion, and (4) adsorption–desorption kinetics. Moreover, the effects of these four microscopic factors are simply additive [34]. For this study, a non-reacting acetone tracer was used, so no broadening effects due to adsorption kinetics are exhibited.

Fortunately, the magnitudes of the first three of these broadening effects can be predicted from separately measured properties. Thus the dimensionless plate height, $h=H/d_p$, which is the height of a theoretical plate divided by the average particle diameter, for a non-adsorbed tracer is given by [33]:

$$h = \frac{2}{\mathrm{Pe}_E} + \frac{(1-u)^2}{3(1-\epsilon_b)}(\mathrm{ReSc}) \cdot \left[\frac{1}{\mathrm{Nu}_{BL}} + \frac{m}{\mathrm{Nu}_{IP}} \right] \quad (2)$$

The major ambiguity in the prediction of the reduced plate height concerns the estimation of the particle-based dispersion Péclet number. For this estimation, the correlation by Gunn [37,38] provides a lower bound, while the correlation by Miller and King [39] represent an upper bound.

Athalye et al. [33], provide means of predicting all of the parameters in Eq. (2). It is only important here to note that none of these parameters contains the direction of flow of percolating fluid. They are thus *invariant* to changes in the direction of flow, and they describe behavior on a size scale of the order of particle diameter. In particular, the convective dispersion term represents the effects of flow disturbances in regions of a size scale similar to d_p.

2.2. Deviations from ideal column behavior

We must now consider the actual flow situation, and we begin by noting that flow in both headers and through the adsorbent bed normally takes place at very low Reynolds number, $\mathrm{Re} << 1$. Such a flow is governed by the creeping flow equation of motion $\nabla^2 v = 0$ and the continuity equation $(\nabla \cdot v) = 0$. Such creeping flows are reversible in that they change sign but not magnitude with the sign of driving pressure. A specific example of such a reversible flow is the Blake–Kozeny equation for flow through porous media [40]:

$$V_0 = \frac{(P_0 - P_L)}{L} \cdot \frac{d_p^2}{150\mu} \cdot \frac{\epsilon_b^3}{(1-\epsilon_b)^2} \quad (3)$$

This equation is only valid for a distance scale that is large in comparison to a diameter of a particle, but small in comparison to the diameter of the column. It follows that flow variations on a large scale, both in the headers and the packing, are reversible, and this is the basis of the reverse-flow technique: if one first pumps fluid through a column in the normal way and then reverses the flow, the effects of macroscopic flow maldistribution will be eliminated in the resulting effluent, now emerging from the former inlet. However any solute pulse broadening caused by the above described microscopic effects will be additive: just twice that occurring at the end of the normal flow period at the point of maximum solvent penetration. This technique becomes particularly powerful if the column behavior is independent of axial position, and this will prove to be the case for the experiments discussed below.

2.3. The method of moments

To take full advantage of the reverse-flow technique one must find a means of characterizing the series system of interest here: a packed section between two headers, and for small columns, two additional regions comprising the peripherals. This problem can be resolved by taking advantage of two simplifying characteristics of our system:

(1) The ability to characterize effluent curves produced by a short tracer pulse in terms of their moments with respect to time, and

(2) The additivity of the moments of greatest interest, as demonstrated by Lightfoot et al. [41].

We introduce the definitions and properties of moments here and defer the problem of curve fitting to the next section. We begin by noting that there are two kinds of moments of interest here:

(1) Absolute moments, defined by:

$$M_n \equiv \frac{\int_{-\infty}^{\infty} c_{\text{eff}} t^n \mathrm{d}t}{M_0} \tag{4}$$

where c_{eff} is the effluent concentration from the system of interest and $M_0 = \int_{-\infty}^{+\infty} c(t)\mathrm{d}t$. The first absolute moment $M_1 \equiv \bar{t}$ defining the mean solute residence time, $\bar{t}$, is the most important.

(2) Central moments are defined by:

$$\mu_n \equiv \frac{\int_{-\infty}^{\infty} c_{\text{eff}} (t - M_1)^n \mathrm{d}t}{M_0} \tag{6}$$

For a Gaussian distribution:

$$\mu_2 = \sigma^2 \tag{7}$$

where σ is the standard deviation of the distribution. This equation then is the origin of Eq. (1) with:

$$\overline{\mu}_2 \equiv \mu_2 / M_1^2 \tag{8}$$

Much of the utility of the method of moments is the additivity of the first absolute moment and the second and third central moments. Thus for our system:

$$M_{1,\text{total}} = M_{1,\text{header}} + M_{1,\text{bed}} \tag{9}$$

$$\mu_{2,\text{total}} = \mu_{2,\text{header}} + \mu_{2,\text{bed}} \tag{10}$$

Realizing that:

$$H_{\text{bed}} = L \cdot \left(\frac{\mu_{2,\text{bed}}}{M_{1,\text{bed}}^2} \right) \tag{11}$$

and

$$M_{1,\text{bed}} = \frac{L}{v_s} \tag{12}$$

Substituting Eq. (12) into Eq. (11), and solving for $\mu_{2,\text{bed}}$ yields:

$$\mu_{2,\text{bed}} = \frac{H_{\text{bed}} L}{v_s^2} \tag{13}$$

Substituting this into Eq. (10) provides:

$$\mu_{2,\text{total}} = \mu_{2,\text{header}} + \frac{H_{\text{bed}}}{v_s^2} \cdot L \tag{14}$$

For this analysis, we will assume that height of a theoretical plate inside the packed bed, $H_{\text{bed,}}$ is independent of the bed depth, L. If a plot of $\mu_{2,\text{total}}$ vs. the bed length, L, gives a linear correlation, one may assume the bed is homogeneous in the direction of flow, and that the y-intercept represents $\mu_{2,\text{header}}$. The third central moment, which describes skewness, is not needed in our analysis.

To quantify the contribution of the two reversible factors of packing inhomogeneity and header maldistribution, one may compare the y-intercept and slope in Eq. (14) for the normal operation with those for the reverse-flow operation. The reverse-flow operation should not show the header effects or effects of macroscopic packing inhomogeneity because their reversible nature causes them to refocus when the direction of flow is reversed. This corresponds to a $\mu_{2,\text{header}}$ of zero, and the height of a theoretical plate inside the packed bed will correspond to the plate height as modeled by the established plate theory. The normal operation will have a non-zero $\mu_{2,\text{header}}$ and a height of a theoretical plate equal to the sum of the plate height based on the microscopic contributions plus a contribution due to packing inhomogeneity. Thus comparison of the slopes of normal operation and reverse-flow will quantify the effects of macroscopic packing heterogeneity, while a comparison of the y-intercepts quantifies the effects of header maldistribution.

3. Experimental

3.1. Experimental procedures

All experiments were performed on a Millipore IsoPak column (I.D. = 44 cm). The column was packed with a Cellufine GC 700 media (mean $d_p = 75$ μm). A schematic drawing of the experimental set-up is shown in Fig. 1. The IsoPak packing skid employs two diaphragm pumps; one transfers the slurry from a holding tank to the IsoPak column, while the other recirculates the slurry in the holding tank to keep a constant slurry concentration. Fig. 2a

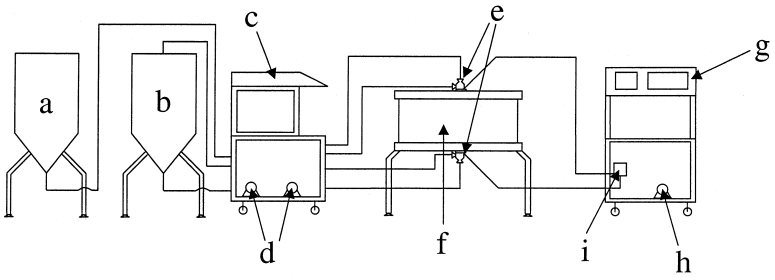

Fig. 1. Schematic of the experimental set-up. a = Liquid vessel; b = slurry vessel; c = IsoPak slurry transfer skid; d = diaphragm pumps for slurry and liquid transfer; e = Millipore IsoPak valves; f = Millipore IsoPak column; g = chromatography system; h = diaphragm pump for chromatographic operation; i = UV detector.

shows the IsoPak column during the packing phase. The slurry enters the column through the IsoPak valve into an unpressurized column initially containing air. The operator can choose whether the slurry is introduced through the valve at the top or the bottom of the column, although the Millipore Operation and Validation Guide [42] recommends introducing the slurry into the bottom of the column and allow removal of air and slurrying buffer through the valve at the top of the column. This technique was employed for every column packed in this study. The top adjuster, containing the top header, could be positioned differently to provide different packing depths. During the packing process, the slurry is pumped at a pressure of 1.5 MPa into the column, pushing the air out through the top valve. Once the column is filled with the slurry, the pumping process continues to feed the slurry into the bottom of the column, while the suspending buffer is pushed out of the top valve into a second holding tank. Once a critical concentration of slurry is reached inside the column, the packed bed begins to form at the top of the column. The packed bed continues to form from the top of the column towards the bottom. The packing process is finished once the pressure inside the column equals the pumping pressure, at which time the diaphragm pump stalls. Fig. 2b illustrates the IsoPak column during the chromatographic operation phase.

Flow reversal was obtained by a series of three-port valves, two before the column inlet and two after the column outlet. These valves were electronically controlled to obtain either flow from the top of the column or flow from the bottom of the column.

All experiments were performed using water purified using a Milli-Q water purification system (Millipore, Bedford, MA, USA) as the mobile phase and slurrying buffer. Differential analysis was per-

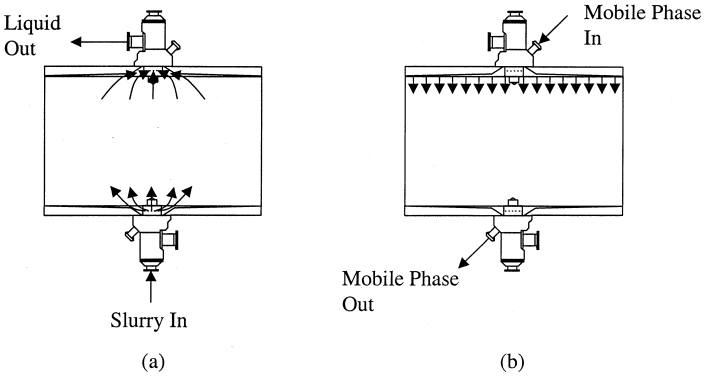

Fig. 2. Millipore IsoPak column (I.D. = 44 cm) and valves. (a) Configuration during the packing process. (b) Configuration during the chromatographic operation process.

formed with 2% (v/v) aqueous HPLC-grade acetone. The pulse size was varied with bed length to assure a consistent effluent response. The feed slurry concentration was varied from 10 to 75% (v/v).

The effluent from the column was analyzed by UV detector operating at 280 nm. The UV signal was then sent electronically to a computer, and all data processing was performed using Microsoft Excel. All data was fitted to a peak shape model, as described below, to obtain the column efficiency as measured by the height of a theoretical plate. The peak shape model was also employed to obtain insight on the unrecorded beginning and end of the effluent peak.

3.2. Data processing

The column efficiency was characterized by evaluating the column response to a pulse of a non-reacting tracer. The solute distribution in the column effluent was described in terms of height of a theoretical plate, as described above.

Fig. 3 shows data for a typical run along with the model prediction used to fit the data. The apparent negative baseline and initial finite slope of the data are artifacts of the data acquisition program. Data was not recorded until the increase in the concentration exceeded a preprogrammed noise level. It was necessary to establish a proper baseline, and this was done by fitting the experimental data to a peak shape model with the concentration baseline as an adjustable parameter and minimizing the sum of squares error between the experimental data and the model-predicted values.

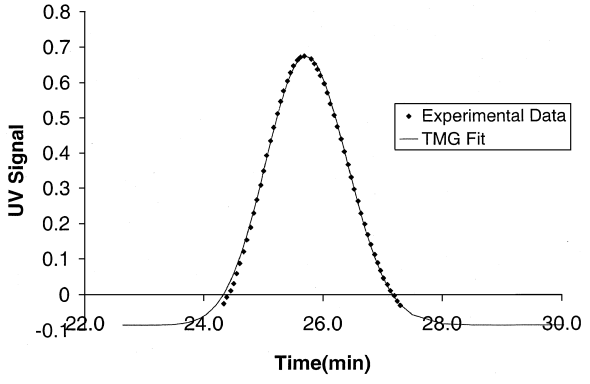

Fig. 3. Comparison of the experimental data to the TMG peak shape model to determine the column efficiency. Points are experimental data, and the solid line represents a TMG fit.

Table 1
Calculation of column efficiency from TMG parameters

μ_0	A
μ_1	$t_G + \frac{\sigma^2}{t_G}$
μ_2	$\sigma^2 + 2 \cdot \frac{\sigma^4}{t_G^2}$

The experimental results were then compared to published predictions of the height of a theoretical plate for well packed columns with ideal flow distribution.

In practice very few effluent curves are truly Gaussian, if only because a finite time is required for the solute band to leave the column. We have therefore fitted our data to a time-modified Gaussian (TMG) model [43], described by:

$$\mathrm{TMG}(t) = \frac{A}{\sqrt{2\pi}\sigma\sqrt{\frac{t}{t_G}}} \cdot \exp\left\{\frac{-(t-t_G)^2}{2\sigma^2\frac{t}{t_G}}\right\} \qquad (15)$$

For this model, A is the peak area, t_G is the time of the peak maximum, and $\sigma\sqrt{\frac{t}{t_G}}$ can be interpreted as the time-dependent variance, in comparison to the Gaussian distribution parameter [43]. Table 1 indicates the determination of the statistical moments from the values of the TMG parameters. Effective numbers of plates, N_{eff}, were then determined from Eq. (1), a procedure justified by the small degree of skewness of the effluent curves. All experimental results have been processed in this way. Except for a few early points, the model fit was satisfactory.

4. Results and discussion

Fig. 3 presents an example of a typical chromatogram obtained from the IsoPak column. All effluent curves showed a slight asymmetry, but this was small enough to allow use of Eq. (1) for fits.

The reproducibility of the IsoPak system was investigated, both in run to run deviations for a given packed column and in deviations from pack to pack, holding the packing conditions constant. Run-to-run

Table 2
Packing reproducibility in the IsoPak packing system[a]

	H (cm)	*N*	*h*
Average	0.0171	1430	2.25
Standard deviation	0.0011	93	0.15

[a] Linear velocity: 50 cm/h, column length: 24 cm.

deviations were shown to be negligible, while pack to pack deviations were small, but significant. Table 2 shows the pack to pack uncertainty in the column efficiency, as measured by the standard deviation of the effective observed number of plates. It may be seen that the variability is small, but observable, with standard deviations of 93 plates out of 1430, or less than 1%.

Table 3 and Fig. 4 present the effect of slurry concentrations on the column efficiency. Slurry concentrations were varied from 10 to 75% (v/v) to examine effects on column efficiency. The supply tank volume limited the lowest concentration that could be studied. It may be seen that there is a shallow optimum, or minimum in the effective height of a theoretical plate for the system, at about 20%. In the range from 75 to 20%, substantial improvement was obtained with decreased slurry concentration. However, below 20%, the column operated less efficiently, and these results were not reproducible. The irreproducibility in this range shows that the column is being packed to a different degree for each pack.

Table 3
Effects of slurry volume fraction on column efficiency[a]

Solid (%)	*N*	*H* (cm)	*h*
10	1320	0.0182	2.42
10	1298	0.0185	2.47
10	1202	0.0200	2.66
15	1327	0.0181	2.41
20	1657	0.0145	1.93
35	1377	0.0174	2.32
53	1280	0.0188	2.50
62	1220	0.0197	2.62
75	989	0.0243	3.24

[a] Linear velocity: 50 cm/h, column length: 24 cm.

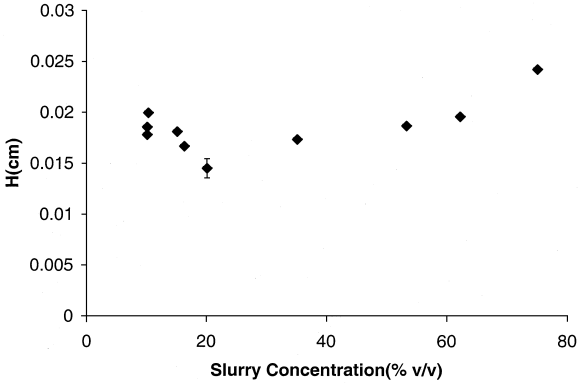

Fig. 4. Effective height of a theoretical plate as a function of the percent of solid media in the packing slurry.

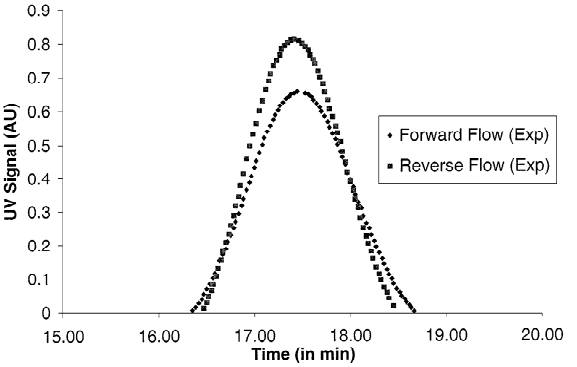

Fig. 5. Comparison of a conventional run under normal operation and a reverse-flow run, where the direction of solvent flow was reversed halfway through the column. Operating conditions are as described in Table 4.

Fig. 5 and Table 4 provide comparisons of a typical conventional run and its reverse-flow counterpart. Almost all of the peak asymmetry exhibited in the conventional run is eliminated when the flow is reversed; the more symmetric peak also provided a decreased H_{eff}. For the forward (normal) flow, the second moment (and thus the height of theoretical plate) is 25% greater than the intrinsic value for the bed alone, which is obtained from the reverse-flow chromatogram.

Table 4
Comparison of column performance under conventional (forward) conditions and under reverse-flow conditions[a]

Flow direction	*N*	*H* (cm)	*h*
Forward flow	1222	0.0131	1.75
Reverse flow	1518	0.0105	1.41

[a] Linear velocity: 50 cm/h, column length: 24 cm.

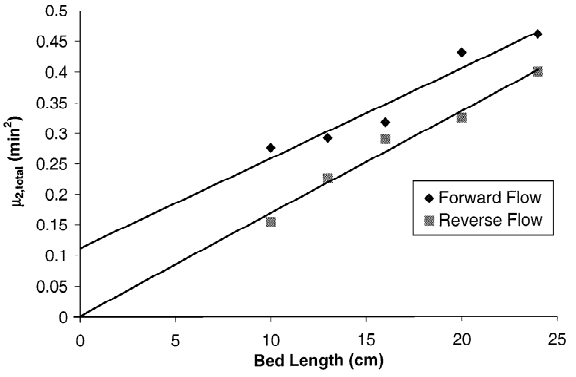

Fig. 6. $\mu_{2,\text{header}}$ vs. bed length. Where replicates were available averages were used.

By varying the depth of the packed bed, and implementing Eq. (14), it is possible to examine the contributions of the packing inhomogeneity and the header maldistribution individually. Fig. 6 and Table 5 show that the slopes of H_{eff} vs. L are not statistically different for conventional and reverse-flow runs. However, there is a substantial intercept for the first while the intercept for the second is not statistically different from zero. We may conclude from this behavior that the packing is indeed homogeneous in the direction of flow and that the intercept represents a significant loss of resolution in the column headers.

The dispersion in the system peripherals was studied by bypassing the column and sending an acetone pulse through the peripherals alone. This peripheral dispersion (0.011 min^2) is an order of magnitude smaller than the dispersion in the header (0.11 min^2), validating the assumption that peripheral dispersion can be neglected in this system. The header dispersion has both direct (inside the header) and indirect contributions. The effects of non-uniform flow distribution from the column headers can cause additional dispersion in the ends of the packed bed until the radial gradients in axial velocity are eliminated. This is header-induced dispersion even though this phenomenon is occurring inside the packed bed.

Table 5
Comparison of forward and reverse flow parameters

Flow direction	$u_{2,\text{header}}$ (min^2)	H_{bed} (cm)
Forward flow	0.11±0.04	0.010±0.002
Reverse flow	0.00±0.03	0.011±0.001

To compare the model prediction for bed behavior with the actual observed behavior, a series of forward-flow tracer pulses were injected in the full length column, and the effective heights of a theoretical plate were calculated from the column effluent. Fig. 7 presents the observed reduced plate height, h, at varying reduced velocities, ReSc. This data is compared to the prediction of the classical one-dimensional chromatographic model. The classical model accounts for the individually additive properties of intraparticle diffusion, mobile phase mass transfer, and axial dispersion. Reduced plate heights of 2–4 were observed over dimensionless velocities in the range of 0 to 20.

For larger molecules, such as proteins, higher reduced velocities will be exhibited; intraparticle diffusion becomes relatively more significant and the range between the two axial dispersion models becomes proportionally smaller, so accuracy of predictions from either model become quite good.

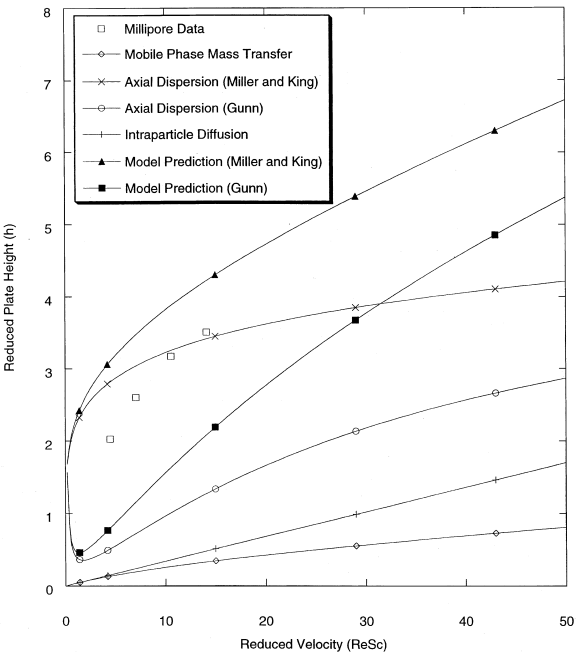

Fig. 7. Comparison of the observed reduced plate height to predicted values for acetone in Cellufine GC 700 media. Error bars not included due to the scale of the graph.

The one-dimensional model, Eq. (2), does not include dispersion from the column headers. The header effects were seen in Fig. 6 to contribute only a small fraction of the second moment for the longest bed depth studied. The reverse-flow experiment clearly demonstrates header dispersion increases the observed second central moment over the intrinsic bed behavior. The increase is 15% as calculated from the linear fits at 24 cm, or 23% if calculated using the value of the header dispersion from the *y*-intercept. If the true plate height were obtained from the reverse-flow experiment, the observed plate height would decrease a corresponding amount, and fall closer to the middle of the model range. However, for shorter beds, where header effects are proportionally larger, this correction must be taken into account or the model prediction will have significant error. For example, Fig. 6 shows that the header contribution to the second central moment of a 10 cm bed length is 50% of the second central moment of the bed alone. Thus the observed overall bed height would also be increased by 50%. For short beds this increase in overall plate heights could readily produce reduced plate heights above the range predicted from the one-dimensional models if header effects are overlooked. Therefore, with short beds and especially with large molecules, consideration of header effects is important in understanding column behavior.

5. Conclusions

This investigation supports a number of conclusions. Most importantly, use of the reverse-flow technique for a series of packed bed depths allows for the quantification of the dispersive effects from macroscopic packing inhomogeneity and header non-uniformities. For a slurry-packed bed using the IsoPak system, a homogeneous packed bed is achieved, with an intrinsic height of a theoretical plate independent of column bed length in the direction of flow. Also, the header flow non-uniformity produces a constant contribution to the second central moment, thus proportionally increasing the observed H_{eff} by up to 50% for the shortest bed length studied, and by relatively smaller amounts for larger bed depths. Lastly, packed bed quality was studied as a function of the particulate fraction of the feed slurry, from 10 to 75% (v/v). This study showed a decrease in column efficiency at both extremes and a relative minimum in plate height at about 20%. These results are being used to plan further studies to understand the general phenomena of bed packing techniques and header non-uniformities.

6. Nomenclature

A	Peak area (arbitrary units)
c_{eff}	Effluent solute concentration (mg/ml)
D_{ip}	Effective solute diffusivity in pore liquid (cm^2/s)
$\bar{D}_{\mathrm{is}}$	Effective solute diffusivity in the percolating solution (cm^2/s)
d_{p}	Diameter of a stationary-phase particle (μm)
E	Convective axial dispersion coefficient (cm^2/s)
ϵ_{b}	Interstitial (interparticle) void fraction in a packed bed
ϵ_{p}	Intraparticle inclusion porosity of a solute
H	Height equivalent to a theoretical plate (HETP) or plate height (cm)
h	Reduced plate height, defined as H/d_{p}
K_{D}	Ratio of solute concentrations in the adsorbent pores and in the external solution at equilibrium
k_{c}	Concentration-based fluid-phase mass-transfer coefficient (cm/s)
k_{p}	Lumped parameter mass-transfer coefficient inside the particle pore (cm/s)
L	Column length (cm)
M_n	n-th absolute moment (s or min)
m	Parameter in the reduced plate height expression, defined as $\frac{D_{\mathrm{is}}}{D_{\mathrm{ip}}} \cdot \frac{1}{\epsilon_{\mathrm{p}} K_{\mathrm{D}}}$
μ	Fluid viscosity (g/cm s)
μ_n	n-th central moment (s^n or min^n)
$\bar{\mu}_n$	Normalized n-th central moment
N	Number of theoretical plates
$\mathrm{Nu}_{\mathrm{BL}}$	Fluid-phase Nusselt number, defined as $k_{\mathrm{c}} d_{\mathrm{p}}/D_{\mathrm{is}}$

Nu_{IP}	Intraparticle Nusselt number, defined as $k_p d_p / D_{ip}$, value 10
Pe_E	Particle-based dispersion Péclet number, defined as $d_p V/E$
P_x	Pressure at position x (atm; 1 atm = 101325 Pa)
Re	Reynolds number, defined as $d_p V\rho/\mu$
ReSc	Reduced velocity or diffusion Péclet number, defined as $d_p V/D_{is}$
ρ	Fluid density (g/cm^3)
σ	Standard deviation of the effluent curve (s or min)
t	Time (s or min)
$\bar{t}$	Mean solute residence time (s or min)
t_G	Time of the peak maximum (s or min)
u	Fraction of solute in the moving fluid phase at long times
V	Magnitude of the interstitial percolating velocity (cm/s or cm/min)
V_0	Superficial velocity, equal to ϵV (cm/s or cm/min)
v	Local fluid velocity (cm/s or cm/min)
v_s	Superficial velocity (cm/s or cm/min)

Acknowledgements

Grateful acknowledgement is given to Dr. Sarah Yuan of Millipore Ltd., Bedford, MA, USA, for helpful comments on the theory and characterization of preparatory-scale columns and to Dr. Vankatesh Natarajan and Ian Rayner of Millipore Ltd., Bioprocess Division, Bedford, MA, USA, for their assistance with the operation of the IsoPak system and Millipore data acquisition system. This research was supported by NSF grant number CTS-95225289 and NSF-GOALI grant number CTS-9900356.

References

[1] M. Kaminski, J. Klawiter, J.S. Kowalcyzk, J. Chromatogr. 243 (1982) 225.
[2] M. Broquaire, J. Chromatogr. 170 (1976) 43.
[3] D. Bar, M. Cande, R. Rosset, Analusis 4 (1976) 118.
[4] T.J.N. Webber, E.M. McKerrell, J. Chromatogr. 122 (1976) 243.
[5] P.A. Bristow, P.N. Brittain, C.M. Riley, B.F. Williamson, J. Chromatogr. 131 (1977) 57.
[6] B.J. Stanley, C.R. Foster, G. Guiochon, J. Chromatogr. A 761 (1997) 41.
[7] F.G. Lode, A. Rosenfeld, Q.S. Yuan, T.W. Root, E.N. Lightfoot, J. Chromatogr. A 796 (1998) 3.
[8] J.C. Sternberg, Adv. Chromatogr. 2 (1966) 205.
[9] J.F.K. Huber, A. Rizzi, J. Chromatogr. 384 (1987) 337.
[10] O. Kalternbrunner, A. Jungbauer, S. Yamamoto, J. Chromatogr. A 760 (1997) 41.
[11] E.J. Fernandez, C.A. Grotegut, G.W. Braun, K.J. Kirshner, J.R. Staudaher, M.L. Dickson, V.L. Fernandez, Phys. Fluids 7 (1995) 468.
[12] A.M. Athalye, Ph.D. Thesis, University of Wisconsin–Madison, Madison, WI, 1993.
[13] E. Bayer, W. Muller, M. Ilg, K. Albert, Agnew. Chem., Int. Ed. Engl. 28 (1989) 1029.
[14] U. Tallarek, E. Baumeister, K. Albert, E. Bayer, G. Guiochon, J. Chromatogr. A 696 (1995) 1.
[15] E. Bayer, E. Baumeister, U. Tallarek, K. Albert, G. Guiochon, J. Chromatogr. A 705 (1995) 37.
[16] Q.S. Yuan, A. Rosenfeld, T.W. Root, D.J. Klingenberg, E.N. Lightfoot, J. Chromatogr. A 831 (1999) 149.
[17] F.G. Lode, MS Thesis, University of Wisconsin–Madison, Madison, WI, 1997.
[18] Q.S. Yuan, Ph.D. Thesis, University of Wisconsin–Madison, Madison, WI, 1999.
[19] B.S. Broyles, R.A. Shalliker, G. Guiochon, J. Chromatogr. A 867 (2000) 71.
[20] R.A. Shalliker, B.S. Broyles, G. Guiochon, Anal. Chem. 72 (2000) 323.
[21] V. Saxena, P. Young, US Pat. 5462659 (1995).
[22] M. LePlang, D. Charbol, US Pat. 5141635 (1992).
[23] R.J. McNeil, US Pat. 4354932 (1982).
[24] A.E. Colvin Jr., M.W. Hanley, US Pat. 4894152 (1990).
[25] M.M. Kearney, K.R. Peterson, T. Vervloet, M.W. Mumm, US Pat. 5354460 (1994).
[26] T. Joseph, A.J. Pearson, R.C. Adams, O.A. Swift, US Pat. 5324426 (1994).
[27] A. Jungbauer, H.P. Letter, US Pat. 5423982 (1995).
[28] L.H. Mott, US Pat. 4399032 (1983).
[29] M.N. Munk, US Pat. 4457846 (1984).
[30] V. Saxena, B.D. Andresen, US Pat. 4865729 (1989).
[31] M. Kaminski, J. Chromatogr. 589 (1992) 61.
[32] D.K. Roper, E.N. Lightfoot, J. Chromatogr. A 702 (1995) 69.
[33] A.M. Athalye, S.J. Gibbs, E.N. Lightfoot, J. Chromatogr. 589 (1992) 71.
[34] A. Klinkenberg, F. Sjenitzer, Chem. Eng. Sci. 5 (1956) 258.
[35] A.J.P. Martin, R.L.M. Synge, J. Biochem. 35 (1941) 1358.
[36] J.J. van Deemter, F.J. Zuiderweg, Chem Eng. Sci. 5 (1956) 271.
[37] D.J. Gunn, Trans. Inst. Chem. Eng. 47 (1969) T351.
[38] D.J. Gunn, Chem. Eng. Sci. 42 (1987) 363.

[39] S.F. Miller, C.J. King, Lawrence Radiation Lab. Rep., UCRL-1191, 1965.
[40] R.B. Bird, W.E. Stewart, E.N. Lightfoot, Transport Phenomena, Wiley, New York, 1960.
[41] E.N. Lightfoot, J.L. Coffman, F. Lode, Q.S. Yuan, T.W. Root, J. Chromatogr. A 760 (1997) 139.
[42] Operating Instructions and Validation Guide: IsoPak Biochromatography Column Pack/Unpack System for IPP and IPS 440, 630, 800, and 1000 Columns, Publication No. 43526WA, Millipore Corporation, Bedford, MA.
[43] J.F.G. Reis, E.N. Lightfoot, P.T. Noble, A.S. Chiang, Sep. Sci. Technol. 14 (1979) 367.